

RESEARCH ARTICLE

## A numerical scheme for the one-dimensional neural field model

Aytül Gökçe<sup>a\*</sup>, Burcu Gürbüz<sup>b</sup>

<sup>a</sup>*Department of Mathematics, Faculty of Science and Arts, Ordu University, Ordu, Turkey*

<sup>b</sup>*Institute of Mathematics, Johannes Gutenberg-University, Mainz, 55128 Germany*  
*aytulgokce@odu.edu.tr, burcu.gurbuz@uni-mainz.de*

---

### ARTICLE INFO

#### Article History:

*Received 24 January 2022*

*Accepted 28 July 2022*

*Available 29 July 2022*

#### Keywords:

*Neural field*

*Integro-differential equation*

*Numerical methods*

#### AMS Classification 2010:

*92B20; 34K28; 37Mxx*

---

### ABSTRACT

Neural field models, typically cast as continuum integro-differential equations, are widely studied to describe the coarse-grained dynamics of real cortical tissue in mathematical neuroscience. Studying these models with a sigmoidal firing rate function allows a better insight into the stability of localised solutions through the construction of specific integrals over various synaptic connectivities. Because of the convolution structure of these integrals, it is possible to evaluate neural field model using a pseudo-spectral method, where Fourier Transform (FT) followed by an inverse Fourier Transform (IFT) is performed, leading to an identical partial differential equation. In this paper, we revisit a neural field model with a nonlinear sigmoidal firing rate and provide an efficient numerical algorithm to analyse the model regarding finite volume scheme. On the other hand, numerical results are obtained by the algorithm.



## 1. Introduction

The cortex has a structure which can be viewed as a great number of macro and micro columns, each of which encapsulates laminar substructures and is considered as an elementary unit of the cortex [1, 2]. Studying columnar organisation of the cortex traces its roots back to a seminal work of Mountcastle in the 20th century, when clusters of neurons, that form cylinders of  $200 - 500\mu m$ , are aligned through cortical layers [1, 3]. The 20th century witnessed two breakthrough that shed lights on the foundations of theoretical neuroscience: (i) large scale cortical dynamics of the cortex relies on the dynamics of individual neurons, (ii) individual neurons can be accounted as electrical units and have an essential role to conduct signals by reacting to electrical current. Therefore the invention of multi-electrode technology provided researchers to characterise the resting state of the membrane voltage of neurons in a cortical tissue. The development of these techniques for cortical tissue had

lead new research manners to analyse the electrophysiological investigations of synaptic transmission [3, 4]. Hence, large-scale spatio-temporal dynamics of neural populations which were not recognised by the scientific community till the 1980s, have been one of the primary sources in theoretical neuroscience.

Neural field models have specifically been investigated to understand the behaviour of a real cortical tissue in space and time. The history of these models is based on Beurle's pioneering work, where the study of masses of cells in the brain considering only excitatory neurons is provided, in the 1950s [5]. The bases of modern versions of these models have been conceived by Wilson and Cowan [6, 7], Amari [8, 9] and Nunez [10] in the late 1970s. Since their initial inception, neural fields have been widely analysed in one and two dimensional systems. This has mostly encapsulated the mathematical investigations and numerical analysis of space-time cortical patterns,

---

\*Corresponding Author

and much has been studied about localised patterns, global periodic states and travelling waves. These tissue level models have shed lights into understanding of many application areas including large-scale brain rhythms [11], geometric visual hallucinations [12], motion perception [13] and short term memory [14]. For more current perspective for the analysis of neural field modelling we refer reader to a comprehensive book by Coombes et al. [15]. Neural field models have been viewed spatially extended models to mimic the macroscopic spatio-temporal dynamics of interacting neurons and written in the form of partial integro-differential equations. Using various synaptic connectivity functions between neurons and firing rate functions, these models are known to support various solutions, e.g. localised structures as well as travelling waves observed in a real cortical tissue. These continuum models have non-local nature and have been widely analysed numerically and analytically. Here we present a numerical scheme to study space-time solutions in neural fields. This provides an alternative aspect to solve the neural field equations given in the form of an integro-differential equation and comparable with its analytical representation.

Here we present an adapted numerical scheme to obtain numerical approximation to the solutions in neural fields. The numerical scheme is based on the finite volume approach and first we describe the discretisation process by working on cell centered and collocated grid of meshes. Then we provide an expression for the numerical fluxes. By the calculation of fluxes, we obtain matricial formulation. On the other hand, an approximation of the average value of  $f$  on the cell is calculated by the Gaussian quadrature. Thereafter, the Patankar matrix is defined in the matricial formulation and the system is solved by a series approach together with the help of control volume.

This chapter is organised as follows. In Sec. 2, we revisit a primer one dimensional neural field model and summarise the previous results. Then, in Sec. 3, an equivalent partial differential equation is derived with a pseudo-spectral method using Fourier Transform (FT) followed by an inverse Fourier transform (IFT). Sec. 3 is dedicated to an efficient numerical algorithm for the neural field model in partial differential equation form with an exponentially decaying synaptic kernel and sigmoidal firing rate function. Lastly, in Sec. 5, summary of the results is given with potential future directions.

## 2. The PIDE model

In this section, we concentrate on a minimal one-dimensional neural field equation that can be written as a partial integro-differential equation (PIDE) of the form

$$\frac{\partial v(x, t)}{\partial t} = -v(x, t) + \int_{\Omega} w(x - y) f(v(y, t) - \kappa) dy, \quad (1)$$

where  $\Omega \subseteq \mathbb{R}$  is a planar domain,  $x \in \Omega$  and  $t \in \mathbb{R}^+$ . Here the variable  $v$  stands for the synaptic activity of neuron population, the function  $w$  represents the anatomical connectivity between neurons and assumed that the connectivity depends on the Euclidean distance  $|x - y|$ . The function  $f$  denotes a sigmoidal type firing rate and the constant parameter  $\kappa$  is the firing threshold.

Typical forms for the connectivity function are often considered using exponential functions such that

$$\lim_{x \rightarrow \infty} w(x) = 0 \quad \text{and} \quad \int_{-\infty}^{\infty} w(x) dx < \infty. \quad (2)$$

Therefore the kernel describing the spatial distribution of synaptic interactions can be chosen in the simplest form of

$$w(x) = \frac{1}{2\sigma} e^{-|x|/\sigma}, \quad (3)$$

where  $w$  is chosen as symmetrical, e.g.  $w(x) = w(-x)$  and continuous, and  $\sigma$  is a scaling parameter. This version of exponentially decaying connectivity function is known to support the generation of travelling front solutions which connects high activity states to a low activity states [16–18].

Besides, the firing rate non-linearity triggered by the membrane voltage is generally chosen in a smooth and monotonically increasing functional form with

$$\lim_{x \rightarrow -\infty} f(v(x, t)) = 0 \quad \text{and} \quad \lim_{x \rightarrow \infty} f(v(x, t)) = 1. \quad (4)$$

Hence, we consider an example form of such firing rate as

$$f(v(x, t) - \kappa) = \frac{1}{1 + e^{-\alpha(v(x, t) - \kappa)}}, \quad (5)$$

where  $\alpha$  represents the steepness parameter and  $\kappa$  is the firing threshold. The form of the synaptic kernel and firing rate function is given in Fig. 1. Studying neural field models with given example of firing rate non-linearity and connectivity often

allows a good understanding of the solutions as given in Fig. 2 and their stability.

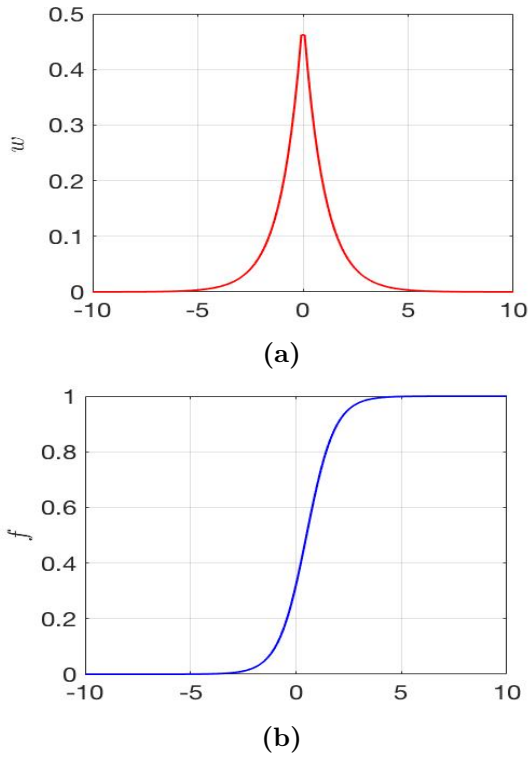


**Figure 1.** The synaptic kernel (a) and sigmoidal firing rate function (b) mimicking the interactions in the brain. Parameters are  $\kappa = 0.5$ ,  $\sigma = 1$  and  $\mu = 1.5$ .

A simplification to the model described in Eq. (1) is made by Amari, who considered a Heaviside choice of firing rate:  $f(u) = H(u - \kappa)$  assuming that  $f(v(x, t)) = 0$  if  $v \leq \kappa$  and  $f(v(x, t)) = 1$  if  $v > \kappa$ . Here  $H$  stands for the Heaviside function. The front solution to neural field model with a Heaviside firing rate has been studied by Coombes *et al.* for interface dynamics [18], where a typical front solution is considered as  $v(x, t) > \kappa$  for  $x < x_0(t)$  and  $v(x, t) \leq \kappa$  for  $x \geq x_0(t)$ . Here  $x_0(t)$  represents the evolution of interface connecting high activity state to a low activity state.

Although partial integro-differential equations (PIDE) for neural field models described in Eq. (1) are thoroughly studied in the literature for various connectivity and firing rate functions, one can also describe an identical equation of partial differential equations (PDE). This link from PIDE form to PDE form of the neural field model can be efficiently used for more straight-forward theoretical and numerical investigations [19, 20]. A large amount of analytical work has been performed on Eq. (1). Although the cortex is actually a two-dimensional domain, it is more realistic to

analyse neuronal system in two dimension. However, here we focus on a one-dimensional primer to explain the numerical algorithm.

### 3. An equivalent PDE model

From now on our attention is directed in two folds. Firstly, using the ideas presented by Laing and Troy [20], we describe PDE which is identical to PIDE given in Eq. (1). Secondly, we provide an efficient numerical solution for the PIDE form. Owing to the convolution structure in Eq. (1), several methods have been developed to convert PIDE form to an equivalent PDE form [14]. One of these methods is applied using a Fourier transform for the convolution of the synaptic kernel and firing rate, manipulate the obtained equation. Then an inverse Fourier Transform is performed to transform the dynamics to an equivalent PDE version of the model in Eq. (1). This technique has been efficiently used to exploit dynamical systems with several standard tools [21, 22], as well as allowing for a numerical analysis of spatio-temporal neural fields in one and two dimensions.

A Fourier Transform of the convolution of synaptic kernel and firing rate functions is described as the product of their Fourier transforms. We now assume that  $v$  and  $v_t$  are continuous and integrable with  $x \in \mathbb{R}$  and  $t \in \mathbb{R}^+$ , and follow the ideas described in [14, 20]. Thus  $FT[v](p)$  can be denoted as the Fourier transform of  $v(x)$  where  $p$  is the transform variable. Here the Fourier transform of the connectivity function  $w$  can be written with a rational function of  $p^2$ , e.g.  $A(p^2)/B(p^2)$ , where  $p$  denotes the Euclidean distance in Fourier space. Using the properties of convolution and applying FT to both sides of Eq. (1):

$$FT \left[ \frac{\partial v}{\partial t} + v \right] = FT[w]FT[f(v - \kappa)], \quad (6)$$

where  $FT[\cdot]$  represents the Fourier transform. Therefore, for the kernel given in Eq. (3), it can be written that

$$FT[w] = \frac{A(p^2)}{B(p^2)} = \frac{1}{1 + \sigma^2 p^2}. \quad (7)$$

Then Eq. (6) can be given as

$$(1 + \sigma^2 p^2)FT \left[ \frac{\partial v}{\partial t} + v \right] = FT[f(v - \kappa)]. \quad (8)$$

Taking the inverse Fourier transform, the model becomes

$$\left(1 - \sigma^2 \frac{\partial^2}{\partial x^2}\right) \left(\frac{\partial v(x, t)}{\partial t} + v(x, t)\right) = f(v(x, t) - \kappa), \quad (9)$$

leading to

$$v_t + v - \sigma^2 v_{txx} - \sigma^2 v_{xx} = f(v - \kappa), \quad (10)$$

where  $f$  is the sigmoidal firing rate nonlinearity given in Eq. (5) and  $\kappa$  is a constant threshold. Here we also used that  $FT[v_{xx}] = -p^2 FT[v]$ . The partial differential equation given in Eq. (10) is an equivalent version of the partial integro-differential equation given in Eq. (1) with synaptic kernel in Eq. (3) and non-linear firing rate in Eq. (5).

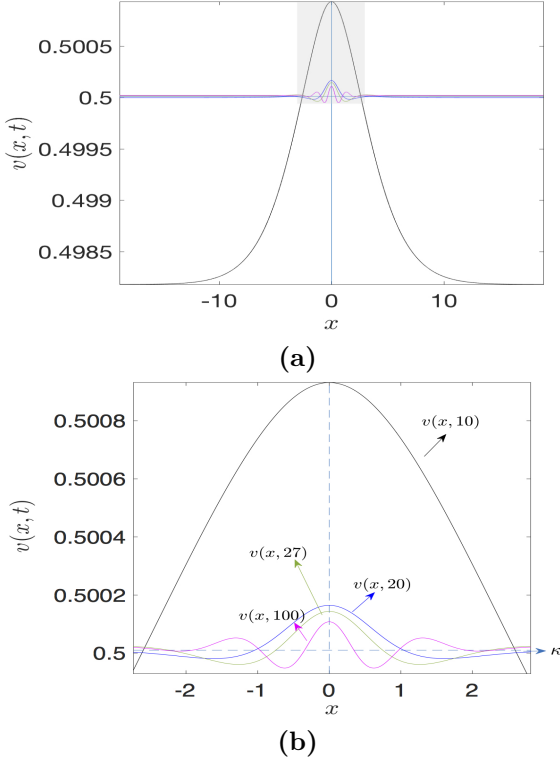


**Figure 2.** A bump solution  $u(x, t)$  at various times:  $t = 10$ (black),  $t = 20$  (blue),  $t = 27$  (green),  $t = 100$  (magenta) is shown in (a). The region that is highlighted with gray in (a) is zoomed in (b). Parameters are  $\kappa = 0.5001$ ,  $\mu = 2.5$ ,  $\sigma = 1$  and the domain size is  $L = 6\pi$ . The initial condition is chosen as  $u(x, 0) = 2/\cosh(x)$ .

In the following section we provide an efficient numerical algorithm based on finite volume approach for solving Eq. (10) with the appropriate conditions. We give detailed information about the numerical approach for the convergence results which is an effective and alternative approximation for such problems [23], [24].

## 4. Numerical investigation

The finite volume method is a well-known numerical approach for describing partial differential equations and to evaluate in the algebraic

equations form. The typical description of the method consists of discretisation process which is for solving the partial differential equations. This is acquired a system of algebraic equations. On the other hand, the discretisation procedure can be applied for a cell centered and collocated grid of meshes depending on a geometrical and mesh construction of the problem. Thus it is clearly visible in the miscellaneous applications of the method that it is of various types of numerical algorithms regarding variable types of the equations and featured operators [25]. The method also express the conservation laws of related to the amount of unknowns in the equation which is namely indicated by the flux. In a specific case, this expression can be satisfied by the synaptic activities in a neural field studies. Namely, the flux which arrives to a control volume through the synaptic connectivity is of the contrary direction of the synaptic connectivity first existed the control volume. Therefore, we understand that the method is applied on real-world scenarios regarding the geometrical construction of the problem. As a specific example in our study, we describe the 1D problem in the neural field which is adapted to the cell centered meshes. Accordingly, the synaptic activity of neuron population in the scenario with a sigmoidal type firing rate and the related parameters can be explained concerning the meshes for the synaptic connectivities on a planar domain.

In this section, we consider the finite volume conceptualisation for the numerical investigation. The aim is to investigate the numerical solution of Eq. (10) with the suitable Dirichlet boundary conditions. Particularly, we consider first the discretisation procedure and we obtain an interpretation for the fluxes. This leads us to figure out a systematic approach for the calculation of the fluxes which is represented by the Patankar matrix in the matricial formulation.

### 4.1. Discretisation

We design the discretisation process on the cell centered grids (see Fig. 3). First we consider  $I \in \mathbb{N}$  and the domain  $\Omega$  has  $I$  cells. The cells are organised by the point-wise structures  $\phi_i := [x_{i-1/2}, x_{i+1/2}]$  for  $i = 1, 2, \dots, N$  with  $x_{i-1/2}$  and  $x_{i+1/2}$ .

Here we generate the figure for a 1D domain which is of the length  $L$  and it is discretised into the same size of  $N_x$  number of cells [26]. The size of the each cell is given as 0.1 and denoted by  $\Delta x_i$ . We contemplate with the cell-centred

finite volume method for the numerical concept. Therefore, we visualise the domain with the position of the cell centered grids where interfaces are given for the cells.

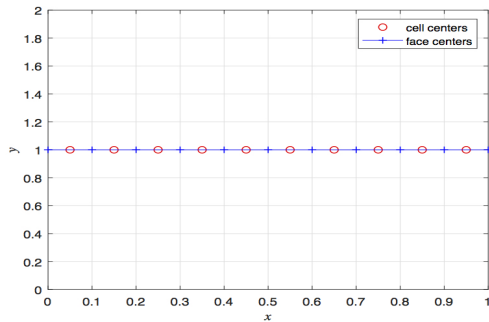


**Figure 3.** The discretised domain in 1D with  $L = 1$  and  $N_x = 10$ .

Now, we design Eq. (10) on cell  $\phi_i$  [27]. We also apply Gauss’s Theorem and transform the equation into the following form [23].

$$\begin{aligned} & \frac{\partial}{\partial t} \int_{\phi_i} v(x, t) dx + \int_{\phi_i} v(x, t) dx \\ & - \sigma^2 \frac{\partial^3}{\partial x^2 \partial t} \int_{\phi_i} v(x, t) dx - \sigma^2 \frac{\partial^2}{\partial x^2} \int_{\phi_i} v(x, t) dx \\ & = f(v(x_{i+1/2}, t) - \kappa) - f(v(x_{i-1/2}, t) - \kappa). \end{aligned}$$

which is alternatively shown as

$$\begin{aligned} & \int_{\phi_i} v(x, t_{n+1}) dx \\ & = \int_{\phi_i} v(x, t_n) dx + \int_{t_n}^{t_{n+1}} f(v(x_{i+1/2}, t) - \kappa) \\ & - \int_{t_n}^{t_{n+1}} f(v(x_{i-1/2}, t) - \kappa), \end{aligned}$$

where  $\Delta t := t_{n+1} - t_n$  is defined for any  $t_n$  and its successive  $t_{n+1}$  in the cell edges for a suitable number  $n$ . Then we divide equation (11) to  $\frac{1}{\Delta x_i}$  where  $\Delta x_i = L$ .

$$\begin{aligned} & \frac{1}{\Delta x_i} \int_{\phi_i} v(x, t_{n+1}) dx = \frac{1}{\Delta x_i} \int_{\phi_i} v(x, t_n) dx \\ & + \frac{1}{\Delta x_i} \left( \int_{t_n}^{t_{n+1}} f(v(x_{i+1/2}, t) - \kappa) \right. \\ & \left. - \int_{t_n}^{t_{n+1}} f(v(x_{i-1/2}, t) - \kappa) \right), \end{aligned}$$

where the numerical scheme is stated for the alternative form as

$$V_i^{n+1} = V_i^n - \frac{\Delta t}{\Delta x_i} (F_{i+1/2}^n - F_{i-1/2}^n), \quad (11)$$

where  $V_i^n$  shows us a new form of the cell averages. It is also an approximation to the average value of  $v$  at anytime  $t^n := n \Delta t$  [28]. Alternatively, we

show

$$\begin{aligned} V_i^n & \approx \frac{1}{\Delta x_i} \int_{x_{i-1/2}}^{x_{i+1/2}} v(x, t_n) dx \equiv \\ & \frac{1}{\Delta x_i} \int_{\phi_i} v(x, t_n) dx. \end{aligned} \quad (12)$$

We denote  $F_{i+1/2}^n$  which is an approximation to the numerical flux through out the cell.

$$F_{i+1/2}^n \approx \frac{1}{\Delta t} \int_{t_n}^{t_{n+1}} f(v(x_{i+1/2}, t) - \kappa). \quad (13)$$

On the other hand, we modify Eq. (11) as in the following form:

$$\frac{V_i^{n+1} - V_i^n}{\Delta t} + \frac{F_{i+1/2}^n - F_{i-1/2}^n}{\Delta x_i} = 0. \quad (14)$$

### 4.2. Numerical flux approximation

The concept of the finite volume method is included approximation to the fluxes. The conservation law is also taken into consideration. The average flux calculation is formulated by the law and also this is counted for the each cell construction [28], [29].

Here we provide an expression for the numerical flux approximation. Let us consider  $x_{i+1/2}$  be an inner interface.

$$F_{i+1/2}^n = \frac{1}{2} [f(V_{i-1}^n) - f(V_i^n)], \quad (15)$$

where we have a formulation for the numerical flux. Now we define the finite volume approach on Eq. (11) and we get

$$F_i^{n+1} = F_i^n - \frac{\Delta t}{2\Delta x_i} [f(V_{i+1}^n) - f(V_{i-1}^n)]. \quad (16)$$

Then we obtain the flux expression and a different version of the expression is written as follows

$$F_i^{n+1} = \frac{1}{2} (F_{i-1}^n - F_{i+1}^n) - \frac{\Delta t}{2\Delta x_i} [f(V_{i+1}^n) - f(V_{i-1}^n)], \quad (17)$$

where  $F_i^n = 1/2(F_{i-1}^n - F_{i+1}^n)$  is the average flux of  $F_{i-1}^n$  and  $F_{i+1}^n$ , respectively. Now we consider the Taylor series of  $v(x, t_{n+1})$  and we get

$$\begin{aligned}
v(x, t_{n+1}) &= v(x, t_n) + \Delta t v_t(x, t_n) \\
&+ \frac{1}{2}(\Delta t)^2 v_{tt}(x, t_n) + \dots \\
&= v(x, t_n) - \Delta t A v_x(x, t_n) \\
&+ \frac{1}{2}(\Delta t)^2 A^2 v_{xx}(x, t_n) + \dots,
\end{aligned}$$

where  $A$  is the matrix which includes constant coefficients. We show the matricial formulation regarding the Taylor series results. Let us consider the first three terms of the series which are from above. We describe an essential equation from the finite difference scheme and we have the following equation [30, 31].

$$\begin{aligned}
V_i^{n+1} &= V_i^n - \frac{\Delta t}{\Delta x_i} A (V_{i+1}^n - V_{i-1}^n) \\
&+ \frac{1}{2} \left( \frac{\Delta t}{2\Delta x_i} \right)^2 A^2 (V_{i-1}^n - 2V_i^n + V_{i+1}^n).
\end{aligned} \tag{18}$$

Now we apply finite volume scheme which is defined in Eq. (11). This gives us a clear statement for the approximation to the fluxes.

$$F_{i-1/2}^n = \frac{1}{2} A (V_{i-1}^n - V_i^n) - \frac{1}{2} \frac{\Delta t}{\Delta x_i} A^2 (V_i^n - V_{i-1}^n). \tag{19}$$

Thus we approximate the flux functions numerically in time  $t_{n+1/2} = t_n + \frac{1}{2}\Delta t$ . Briefly, we have

$$F_{i-1/2}^n = f(V_{i-1/2}^{n+1/2}). \tag{20}$$

For the cell centered and collocated grid of mesh, we have the form of  $V_{i-1/2}^{n+1/2}$  at  $\frac{1}{2}\Delta x_i$  and  $\frac{1}{2}\Delta t$  as follows:

$$V_{i-1/2}^{n+1/2} = \frac{1}{2} (V_{i-1}^n + V_{i+1}^n) - \frac{1}{2} \frac{\Delta t}{\Delta x_i} [f(V_{i+1}^n) - f(V_{i-1}^n)].$$

Now we reduce the system and consider Eq. (11). By applying the upwind method we have

$$V_i^{n+1} = V_i^n - \frac{\bar{\beta} \Delta t}{\Delta x_i} (V_{i+1}^n - V_i^n),$$

and we also have

$$F_{i-1/2}^n = \bar{\beta}^- V_i^n + \bar{\beta}^+ V_{i-1}^n,$$

where  $\beta$  is a constant and  $[\bar{\beta}]^- = \min(\bar{\beta}, 0)$  and  $[\bar{\beta}]^+ = \max(\bar{\beta}, 0)$ . Therefore we define the implicit form of the Patankar matrix  $\mathbf{A} = [A_{ij}]$  [32],

[33], [34].

$$\mathbf{A} = \begin{cases} V_{i-1}^{n+1} - V_{i-1}^n + \frac{\bar{\beta} \Delta t}{\Delta x_i} (V_i^n - V_{i-1}^n) \\ \text{for } j = i - 1, \\ V_i^{n+1} - V_i^n + \frac{\bar{\beta} \Delta t}{\Delta x_i} (V_{i+1}^n - V_i^n) \\ \text{for } j = i, \\ V_{i+1}^{n+1} - V_{i+1}^n + \frac{\bar{\beta} \Delta t}{\Delta x_i} (V_{i+2}^n - V_{i+1}^n) \\ \text{for } j = i + 1, \\ 0, \quad \text{otherwise.} \end{cases}$$

Besides, we define the vectors:

$$\begin{aligned}
\mathbf{V} &= [v_1 \quad v_2 \quad \dots \quad v_N]^T, \\
\mathbf{B}_1 &= [f_1 \quad f_2 \quad \dots \quad f_N]^T, \\
\mathbf{B}_2 &= [k_1 \quad \dots \quad k_{N-1} \quad k_N]^T,
\end{aligned}$$

where  $\mathbf{V}$  is the vector of unknowns,  $\mathbf{B}_1$  is defined for the  $f$  function values and  $\mathbf{B}_2$  is the vector of conditions. Consequently, we solve the system  $\mathbf{A}\mathbf{V} = \mathbf{B}_1 + \mathbf{B}_2$  by using Gaussian Elimination and we obtain the numerical results [35, 36].

### 4.3. Convergence results

In this section, we consider the stability, consistency, and convergence of the method and implement numerical results of Eq. (10) with Dirichlet boundary conditions [37], [38], [39]. We show the difference between the approximate solution and the exact solution by the following statement.

**Definition (local truncation error):** Suppose that the approximate solution of the problem in (10) is replaced by the exact solution. Then by the help of  $\Delta x_i$ , we obtain

$$\tau_i = \frac{1}{\Delta x_i^2} [v_{i-1} - 2v_{i-1} + v_{i+1} - f_i(v - \kappa)], \tag{21}$$

which is the local truncation error for the approximation. The alternative representation is shown by applying the Taylor series expansion [38] and (21) becomes

$$\tau_i = \frac{1}{12} \Delta x_i^2 v_i''' + \mathcal{O}(h^4), \tag{22}$$

where  $\tau_i = \mathcal{O}(h^2)$  as  $h \rightarrow 0$  [38]. Now, we consider the following statement for the stability of the method [40].

**Theorem 1.** *The numerical scheme is considered as stable to solve the problem which is defined in together with the Dirichlet boundary conditions.*

**Proof.** The proof can be found in Section 8, LeVeque, R. J. (2002) [39].  $\square$

We also present the consistency of the method by  $\|\tau^h\| \rightarrow 0$  as  $h \rightarrow 0$  where  $\|\tau^h\| = \mathcal{O}(h^p)$  for  $h = \Delta x_i$  in  $p$ -Norm and the method is considered as consistent by this approach [38]. Besides,

we apply the discretisation on the cell centered and collocated grid of meshes. The numerical calculation of the fluxes gives us an understanding on matricial formulation of the implicit Patankar matrix and we have series approach to obtain the numerical solution. Briefly, the numerical algorithm is applied for the solution of the problem in this direction [41], [42]. We also apply  $L^1$  error,  $E_N = \frac{\sum_{i \in \epsilon_{el}} |v_i^N - v_i^n| |\phi_i|}{\sum_{i \in \epsilon_{el}} |v_i^n| |\phi_i|}$ , and the error in  $L^\infty$  norm,  $E_N = \frac{\sum_{i \in \epsilon_{el}} |v_i^N - v_i^n|}{\sum_{i \in \epsilon_{el}} |v_i^n|}$ , respectively. where  $\epsilon_{el}$  is the cell index set,  $v_i^n$  and  $v_i^N$  are the cell mean values of exact and approximation, respectively [41] at  $t = t_{final}$ . In the case the exact solution is not given, we describe truncation error which supports the finding for the comparison formula in  $L^1$  and  $L^\infty$  norms.

We apply the procedure on Eq. (10) together with the Dirichlet boundary conditions given as 0 at  $t = t_{final}$  and the parameters are given as  $\kappa = 0.5$ , and  $\sigma = 1$ .

**Table 1.**  $L^1$  and  $L^\infty$  convergence results at  $x = 0.2$ .

N	$L^1$ error	$L^\infty$ error
5	0.2514e-04	0.3509e-05
10	0.6004e-05	0.7420e-06
25	0.5038e-06	0.4081e-07
50	0.2203e-06	0.1295e-08

**Table 2.**  $L^1$  and  $L^\infty$  convergence results at  $x = 0.5$ .

N	$L^1$ error	$L^\infty$ error
5	0.2110e-04	0.3172e-05
10	0.5312e-05	0.7359e-06
25	0.4012e-06	0.4019e-07
50	0.1207e-07	0.1260e-08

Numerical results are obtained by MATLAB and Maple computer programs which show us the approximation in details. As we can see in the Table (1), (2), and (3) the approximation gives us more suitable results when the iteration increases. More specifically, we have efficient results after N=5 iteration which gives us an understanding about the performance result of the numerical scheme.

**Table 3.**  $L^1$  and  $L^\infty$  convergence results at  $x = 1.0$ .

N	$L^1$ error	$L^\infty$ error
5	0.1003e-04	0.2113e-05
10	0.4072e-05	0.5087e-06
25	0.2843e-06	0.2809e-07
50	0.0927e-07	0.0891e-08

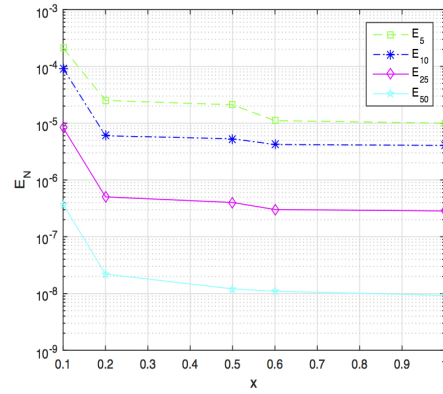


**Figure 4.**  $L^1$  convergence results at  $x = [0, 1]$  for  $N = 5, 10, 25,$  and  $50$ .

On the other hand, Figure 4 shows us  $L^1$  error results and we have decreasing error values by space. In the approximation we consider the analytical findings comparison with the numerical scheme result for our particular case. Figure 5 presents  $L^\infty$  error findings which is of similar effect regarding increasing  $x$  values at the final time.

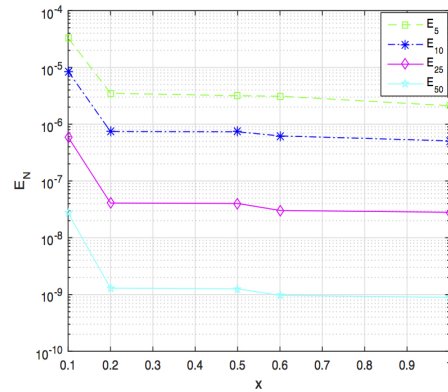


**Figure 5.**  $L^\infty$  convergence results at  $x = [0, 1]$  for  $N = 5, 10, 25,$  and  $50$ .

### 5. Conclusion

In this paper, we revisited a well known neural field model with a sigmoidal firing rate. We firstly provided some biological and theoretical background for the neural field model and summarised a numerical algorithm for partial differential equations. Using the ideas previously presented by Laing [14, 20], the technique to transform partial integro-differential equation to an equivalent form of partial differential equation is applied using Fourier transform followed by an inverse Fourier transform. Considering the equivalent PDE form and setting  $v_t = 0$ , stationary bump solutions of (1) can be obtained. Here, an exponentially decaying connectivity function and sigmoidal firing rate are taken into account for

the convolution integral, see Fig. 1. The spatial derivatives in new form of the neural field model given by Eq. (9) can be computed using finite difference methods in the  $x$  direction. The system given in Eq. (9) is solved in terms of a one dimensional Mass matrix  $M$ , e.g. in the form of  $Mu' = F(u)$  that allows user to compute matrix inverse in MATLAB. The PIDE model given in Eq. (1) and PDE model given in Eq. (9) are equivalent.

The numerical approach for the solution of neural fields used in this paper is based on the finite volume method which encapsulates a discretisation process to solve partial differential equation. Depending on the geometrical structure of the problem, a cell centered and collocated grid of meshes can be used for the discretisation. This approach is complemented with the Patankar matrix in the matricial formulation for the numerical investigation. As seen from the convergence results given in Figs. 4 and 5, numerical approach presented in this paper may provide an alternative direction to solve one dimensional neural fields with a better approximations when iteration increases. One straightforward extension of this work would be to consider adaptation [43,44]. In fact, the experiments carried on cortical tissues imply that there are many metabolic processes that restrain the excitatory dynamics of neural networks. This processes differ from inhibition and called as spike frequency adaptation. The linear adaptation has been a popular modulation for investigating neural response in mean field models. Thus the numerical investigation used in this paper can be extended to include a two component neural field model including synaptic activity of a neuron population and spike frequency adaptation, see [16, 19, 20]. Another possible extension would be a numerical investigation of a two dimensional neural field model. In fact, cortex is a two dimensional structure with a few millimeter thickness. Due to its laminar organisation, the cortex is usually regarded as a two dimensional structure. Therefore it is significant to revisit a two dimensional version of the model and determine the conditions to apply the numerical investigation used here. On the other hand, the numerical investigation of a two dimensional neural field model with and without adaptation may be computationally expensive and challenging to perform in terms of algebraic equations resulting from numerical method.

## Acknowledgments

Aytül Gökçe was supported by BAP (Scientific Research Projects Coordination Unit), Ordu University, through Grant No. A-2007.


## References

- [1] Horton, J. C., & Adams, D. L. (2005). The cortical column: a structure without a function. *Philosophical Transactions of the Royal Society B: Biological Sciences*, 360(1456), 837-862.
- [2] DeFelipe, J., Markram, H., & Rockland, K. S. (2012). The neocortical column. *Frontiers in Neuroanatomy*, 6, 22.
- [3] Mountcastle, V. B. (1957). Modality and topographic properties of single neurons of cat's somatic sensory cortex. *Journal of Neurophysiology*, 20(4), 408-434.
- [4] Martin, R. (2019). *Neuroscience Methods: A Guide for Advanced Students*. CRC Press.
- [5] Beurle, R. L. (1956). Properties of a mass of cells capable of regenerating pulses. *Philosophical Transactions of the Royal Society of London. Series B, Biological Sciences*, 55-94.
- [6] Wilson, H. R., & Cowan, J. D. (1972). Excitatory and inhibitory interactions in localized populations of model neurons. *Biophysical Journal*, 12(1), 1-24.
- [7] Wilson, H. R., & Cowan, J. D. (1973). A mathematical theory of the functional dynamics of cortical and thalamic nervous tissue. *Kybernetik*, 13(2), 55-80.
- [8] Amari, S. I. (1975). Homogeneous nets of neuron-like elements. *Biological Cybernetics*, 17(4), 211-220.
- [9] Amari, S. I. (1977). Dynamics of pattern formation in lateral-inhibition type neural fields. *Biological Cybernetics*, 27(2), 77-87.
- [10] Nunez, P. L. (1974). The brain wave equation: a model for the EEG. *Mathematical Biosciences*, 21(3-4), 279-297.
- [11] Coombes, S. (2010). Large-scale neural dynamics: simple and complex. *NeuroImage*, 52(3), 731-739.
- [12] Ermentrout, G. B., & Cowan, J. D. (1979). A mathematical theory of visual hallucination patterns. *Biological Cybernetics*, 34(3), 137-150.
- [13] Giese, M. A. (2012). *Dynamic neural field theory for motion perception (Vol. 469)*. Springer Science & Business Media.
- [14] Laing, C. R. (2014). PDE Methods for Two-Dimensional Neural Fields. In *Neural Fields* (pp. 153-173). Springer, Berlin, Heidelberg.




- [15] Coombes, S., beim Graben, P., Potthast, R., & Wright, J. (Eds.). (2014). *Neural Fields: Theory and Applications*. Springer.
- [16] Ermentrout, G. B., & McLeod, J. B. (1993). Existence and uniqueness of travelling waves for a neural network. *Proceedings of the Royal Society of Edinburgh Section A: Mathematics*, 123(3), 461-478.
- [17] Coombes, S. (2005). Waves, bumps, and patterns in neural field theories. *Biological Cybernetics*, 93(2), 91-108.
- [18] Coombes, S., Schmidt, H., & Bojak, I. (2012). Interface dynamics in planar neural field models. *Journal of Mathematical Neuroscience*, 2(1), 1-27.
- [19] Gokce, A. (2017). *The interfacial dynamics of Amari type neural field models on finite domains*. (Doctoral dissertation, University of Nottingham).
- [20] Laing, C. R., & Troy, W. C. (2003). PDE methods for nonlocal models. *SIAM Journal on Applied Dynamical Systems*, 2(3), 487-516.
- [21] Laing, C. R. (2005). Spiral waves in nonlocal equations. *SIAM Journal on Applied Dynamical Systems*, 4(3), 588-606.
- [22] Coombes, S., beim Graben, P., Potthast, R., & Wright, J. (Eds.). (2014). *Neural Fields: Theory and Applications*. Springer.
- [23] Fedak, A. (2018). *A compact fourth-order finite volume method for structured curvilinear grids*. University of California, Davis.
- [24] Cueto-Felgueroso, L. (2009). *Finite volume methods for one-dimensional scalar conservation laws*. <http://juanegroup.mit.edu/lcueto/teach>.
- [25] Zoppou, C., Knight, J. H. (1999). Analytical solution of a spatially variable coefficient advection-diffusion equation in up to three dimensions. *Applied Mathematical Modelling*, 23(9), 667-685.
- [26] Eftekhari, A.A. et al. (2015). FVTool: a finite volume toolbox for Matlab. Zenodo. <http://doi.org/10.5281/zenodo.32745>
- [27] Nordbotten, J. M. (2014). Cell-centered finite volume discretizations for deformable porous media. *International Journal for Numerical Methods in Engineering*, 100(6), 399-418.
- [28] Mungkasi, S. (2008). *Finite volume methods for the one-dimensional shallow water equations*. (M. Math. Sc. thesis, Australian National University).
- [29] Eymard, R., Gallouët, T., Herbin, R., Latché, J. C. (2007). Analysis tools for finite volume schemes. *Proceedings of Equa Diff* 11, 111-136.
- [30] Versteeg, H. K., Malalasekera, W. (2007). *An introduction to computational fluid dynamics: the finite volume method*. Pearson Education.
- [31] Abbott, M. B., Basco, D. R. (1997). *Computational fluid dynamics: an introduction for engineers*. Longman.
- [32] Patankar, S. V. (1991). *Computation of conduction and duct flow heat transfer*. CRC Press.
- [33] Patankar, S. V. (2018). *Numerical heat transfer and fluid flow*. CRC Press.
- [34] Patankar, S. V. (1981). A calculation procedure for two-dimensional elliptic situations. *Numerical Heat Transfer*, 4(4), 409-425.
- [35] Evans, L.C. (2010). *Partial differential equations*. American Mathematical Society, Providence, Rhode Island.
- [36] Anderson, J. D., Wendt, J. (1995). *Computational fluid dynamics* (Vol. 206, p. 332). New York: McGraw-Hill.
- [37] Morton, K. W., & Mayers, D. F. (2005). *Numerical solution of partial differential equations: an introduction*. Cambridge University Press.
- [38] LeVeque, R. J. (2007). *Finite difference methods for ordinary and partial differential equations: steady-state and time-dependent problems*. Society for Industrial and Applied Mathematics.
- [39] LeVeque, R. J. (2002). *Finite volume methods for hyperbolic problems* (Vol. 31). Cambridge university press.
- [40] Badr, M., Yazdani, A., & Jafari, H. (2018). Stability of a finite volume element method for the time-fractional advection-diffusion equation. *Numerical Methods for Partial Differential Equations*, 34(5), 1459-1471.
- [41] Syrakos, A., Goulas, A. (2006). Estimate of the truncation error of finite volume discretization of the Navier-Stokes equations on collocated grids. *International journal for numerical methods in fluids*, 50(1), 103-130.
- [42] Fraysse, F., de Vicente, J., Valero, E. (2012). The estimation of truncation error by  $\tau$ -estimation revisited. *Journal of Computational Physics*, 231(9), 3457-3482.
- [43] Ermentrout, G. B., Folias, S. E., & Kilpatrick, Z. P. (2014). Spatiotemporal pattern formation in neural fields with linear adaptation. In *Neural Fields* (pp. 119-151). Springer, Berlin, Heidelberg.
- [44] Benda, J., & Herz, A. V. (2003). A universal model for spike-frequency adaptation. *Neural Computation*, 15(11), 2523-2564.

**Aytül Gökçe** is a Research Fellow at Ordu University in Turkey, working in the broad area of applied mathematics. Aytül's research is mainly devoted to dynamical systems modelling in biology and medicine, and the understanding of patterning in real life problems.

 <https://orcid.org/0000-0003-1421-3966>

research interests ordinary and partial differential equations, integral and integro differential-difference equations, dynamical systems and their analysis, numerical methods, mathematical biology and scientific computation.

 <https://orcid.org/0000-0002-4253-5877>

**Burcu Gürbüz** is a Research Associate in Johannes Gutenberg-University Mainz in Germany. Her main

An International Journal of Optimization and Control: Theories & Applications (<http://ijocta.balikesir.edu.tr>)



This work is licensed under a Creative Commons Attribution 4.0 International License. The authors retain ownership of the copyright for their article, but they allow anyone to download, reuse, reprint, modify, distribute, and/or copy articles in IJOCTA, so long as the original authors and source are credited. To see the complete license contents, please visit <http://creativecommons.org/licenses/by/4.0/>.